Environ Monit Assess (2022) 194: 512
https://doi.org/10.1007/s10661-022-10152-2

Evaluation of thermal infrared imaging from uninhabited aerial vehicles for arboreal wildlife surveillance

Blair Mirka · Douglas A. Stow · Gernot Paulus · Andrew C. Loerch · Lloyd L. Coulter · Li An · Rebecca L. Lewison · Lena S. Pflüger

Received: 1 December 2021 / Accepted: 28 May 2022 / Published online: 17 June 2022

Abstract An important component of wildlife management and conservation is monitoring the health and population size of wildlife species. Monitoring the population size of an animal group can inform researchers of habitat use, potential changes in habitat and resulting behavioral adaptations, individual health, and the effectiveness of conservation efforts. Arboreal monkeys are difficult to monitor as their habitat is often poorly accessible and most monkey species have some degree of camouflage, making them hard to observe in and below the tree canopy. Surveys conducted using uninhabited aerial vehicles (UAVs) equipped with thermal infrared (TIR) cameras can help overcome these limitations by flying above the canopy and using the contrast between the warm body temperature of the monkeys and the cooler background vegetation, reducing issues with impassable terrain and animal camouflage. We evaluated the technical and procedural elements associated with conducting UAV-TIR surveys for arboreal and terrestrial macaque species. Primary imaging missions and analyses were conducted over a monkey park housing approximately 160 semi-free-ranging Japanese macaques (*Macaca fuscata*). We demonstrate Repeat Station Imaging (RSI) procedures using co-registered TIR image pairs facilitate the use of image differencing to detect targets that were moving during rapid sequence imaging passes. We also show that 3D point clouds may be generated from highly overlapping UAV-TIR image sets in a forested setting using structure from motion (SfM) image processing techniques. A point cloud showing area-wide elevation values was generated from TIR imagery, but it lacked sufficient point density to reliably determine the 3D locations of monkeys.

Keywords Drone · RSI · SfM · Change detection · Monkey

B. Mirka (✉) · D. A. Stow · A. C. Loerch · L. L. Coulter · L. An
Department of Geography, San Diego State University, San Diego, CA, USA
e-mail: bmirka@unm.edu

G. Paulus
Spatial Information Management, Carinthia University of Applied Sciences, Villach, Austria

L. An
Center for Complex Human-Environment Systems, San Diego State University, San Diego, CA, USA

R. L. Lewison
Department of Biology, San Diego State University, San Diego, CA, USA

L. S. Pflüger
Department of Behavioral and Cognitive Biology, University of Vienna, Vienna, Austria

L. S. Pflüger
Austrian Research Center for Primatology, Ossiach, Austria

Introduction

Monitoring the population size and density of a species is an important component of wildlife ecology management and conservation. For nonhuman primates, traditional methods of monitoring animal populations have relied on ground-based line transects (Campbell et al., 2016; Plumptre et al., 2013). These methods involve multiple ground-based observers walking through a study area and conducting a manual count of the target animals. This process can be labor-intensive and may require observers to walk long distances through difficult terrain and vegetation. Additionally, achieving accurate animal counts is impeded if the animals being observed flee when approached or are located outside of the researchers' field of view. This is a concern when attempting to detect arboreal monkeys which are easily obscured by vegetation and may retreat from the surveyor's line of sight when approached.

Recent advances in uninhabited aerial vehicles (UAVs), small lightweight thermal-infrared (TIR) imaging sensors, and image geometric processing techniques have created the opportunity for ecologists and wildlife scientists to survey larger areas at reduced costs compared to conventional ground-based surveillance. UAV-TIR systems enable high temporal and spatial resolution imaging of heat-related emissions that tend to have a greater target to background contrast than surface reflectance values, which have the potential to greatly increase the accuracy and reliability of wildlife counts. Previous studies have attempted to determine optimal UAV survey flight parameters (Gonzalez et al., 2016; Oishi et al., 2018; Witczuk et al., 2018), with a recent surge in research on UAV-TIR imaging for the detection of arboreal wildlife evident in the remote sensing and wildlife conservation literature (Burke et al., 2019; He et al., 2020; Kays et al., 2019; Spaan et al., 2019; Zhang et al., 2020).

The pioneering studies cited above have primarily demonstrated that UAV-TIR systems can detect arboreal monkeys and can be used to estimate wildlife populations. The novelty of the research conducted for this study is the implementation of rapid change detection and SfM modeling, which provides additional information about animal movement and positioning within the canopy.

SfM is a photogrammetric technique that uses computer vision-based algorithms to model three-dimensional (3D) structures from dense overlapping image frame datasets. SfM methods work by identifying matching features within overlapping imagery and use the associated parallax information as input for highly redundant bundle adjustments. Camera positions and scene geometries are simultaneously solved, and a sparse 3D point cloud is generated (Westoby et al., 2012). Prior research using SfM processing with TIR imagery has focused on active volcanoes (Thiele et al., 2017), measuring the relative temperature distribution of a building envelope structure (Zheng et al., 2020), and modeling forest canopies (Webster et al., 2018). However, we are not aware of past research that focused on identifying wildlife in 3D models generated with UAS-TIR imagery and SfM approaches.

Image registration and change detection are enhanced by an approach called RSI (Coulter et al., 2015; Loerch et al., 2018; Stow et al., 2016). RSI involves capturing images over time from nearly the same aerial camera station and then registering, enhancing, or detecting changes on a frame-by-frame basis. This approach reduces noise and false detections associated with image misregistration and can detect moving features when images are captured in rapid sequence (Stow et al., 2014). RSI has been implemented with both piloted and unpiloted aerial imagery (Coulter et al., 2015; Stow et al., 2016) and has the potential to increase the accuracy of animal population estimates by being able to monitor animals in motion through highly overlapping imagery and change detection.

In addition to the accuracy and efficiency of animal observation, an important concern when conducting UAV-based wildlife surveys is monitoring and limiting wildlife disturbance and adverse reactions to overflying UAVs. Previous studies show that animals can exhibit both behavioral (Pomeroy et al., 2015; Mulero-Pázmány et al., 2017) and physiological (Ditmer et al., 2015; Vas et al., 2015) responses that can have negative consequences on animal welfare. The low altitude and loud buzzing noise emitted from a UAV can cause animals to respond in a "flight or fight" response, which can disrupt their natural behavior (Ditmer et al., 2015; Pomeroy et al., 2015; Mulero-Pázmány et al., 2017).

This study focuses on the technical and procedural elements of using UAV-TIR remote sensing to conduct arboreal animal surveys. The objective is to test the applicability of new technologies for animal surveying and to refine current TIR imaging approaches toward achieving greater animal survey proficiency in forested areas. Another objective is to explore the potential to estimate the three-dimensional positions of arboreal animals and surrounding vegetation canopies and ground-level utilizing SfM photogrammetric techniques applied directly to UAV-TIR image sets. We consider how the welfare of arboreal species might be impacted by UAV presence and how to minimize such impacts. The research questions addressed in this study are as follows:

1. What flight parameters (e.g., flight pattern, flight speed, and flight elevation) yield reliable arboreal monkey detection?
2. How does monkey detection using TIR imagery compare to conventional RGB imagery?
3. What role can the rapid sequence RSI approach play in improving the accuracy and information content of arboreal monkey surveys?
4. How well do 3D surface models generated by applying SfM processing to overlapping UAV-TIR imagery represent arboreal landscapes and animals within and below tree canopies?

Methods

Initial testing for this study was focused on establishing optimal flight parameters and monitoring monkey responses to UAV overflights. Once these parameters were determined and it was decided that there was minimal risk of adverse monkey reaction at the chosen flight altitude, an imaging flight was conducted, which resulted in an image dataset that was used for TIR and RGB 3D models and monkey detection and validation from the high-resolution RGB imagery. An additional flight provided imagery that was used for RSI-based image registration and change detection analysis. Figure 1 provides an overview of the work process.

Data collection

Multiple UAV imaging missions were conducted to test and select appropriate flight parameters, such as ground speed altitude, image trigger rate, radiometric settings, and the time of day, in the context of detecting thermal targets. Initial tests were conducted in

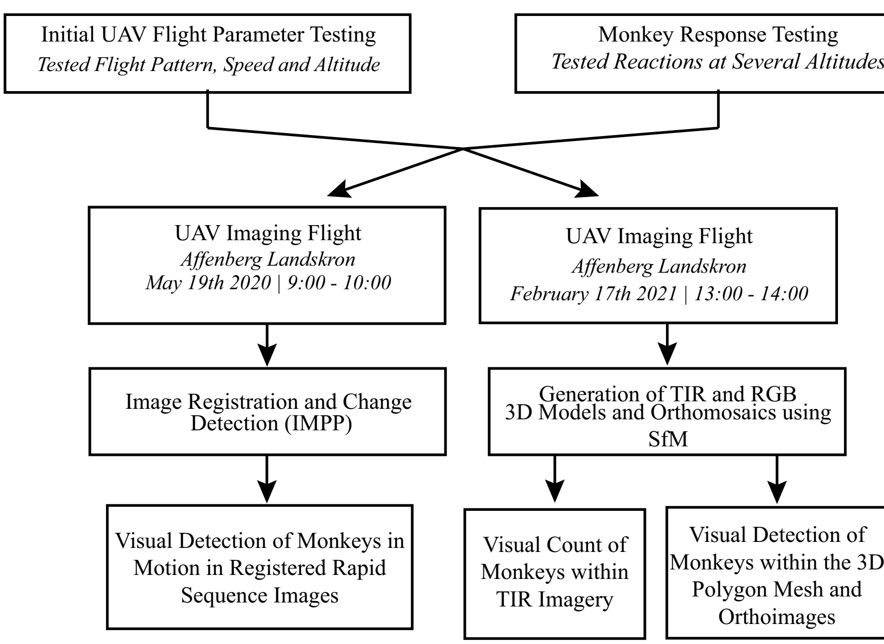

Fig. 1 Overview of research workflow showing the function of the two datasets and the processing goals for each image set

open areas with people serving as targets to establish a baseline for detectability. The complexity of the scene increased in subsequent testing by selecting sites with denser foliage and canopy cover while also working toward detecting monkeys, which are smaller thermal targets. Test sites included a model airplane field and unmaintained low stature grass fields (MFG Feistritz Gail near Villach, Austria) and a small creek with sparse riparian tree and shrub vegetation (Alvarado Creek, San Diego, CA, USA), and a densely forested monkey park Affenberg Landskron (Affenberg Zoobetriebsgesellschaft mbH, field research station, University of Vienna), near Villach, Austria (referred to throughout as either Affenberg or "the monkey park" and was the primary test site for UAV-based monkey detection). Table 1 provides an overview of each of the flights, including the testing environment, date, time, flight altitude, UAV, and camera(s) used.

The size and noise level of tested UAVs were taken into consideration when conducting flights over monkeys as larger and louder UAVs were more likely to be noticed and potentially cause stress and negative reactions from monkeys. The size of the UAV was based on the unfolded dimensions of the aircraft, including propellers and frame arms. Later tests at the monkey park site were conducted at higher altitudes as TIR cameras with higher spatial resolution became available (see Table 1 for details).

Based on initial test flights, the imaging missions were designed to be minimally invasive, using higher flight altitudes and in coordination with experts from the center that could help monitor monkey reactions. All flights were conducted with a minimum 70% sequential image forward and sideward overlap following repetitive "lawnmower" or "racetrack" flight patterns. This high percentage overlap is necessary

Table 1 Specifications for pre-imaging flights conducted throughout this study as well as the imaging flights used for the final analysis (Abenteuer Affenberg (3) and Abenteuer Affenberg (4))

Test area	Date	Time	Altitude(s) Above ground level	UAV	Camera
MFG Feistritz Gail	June 16, 2019	09:23–09:39	40 m	Leica Aibot AX20	FLIR Duo R 160 × 120 pixels
Unmaintained field	June 14, 2019	07:26–07:36	20 m, 40 m, 60 m	Leica Aibot AX20	FLIR Duo R 160 × 120 pixels
Low grass field (1)	July 3, 2019	07:30–07:48	30 m, 40 m, 50 m	Leica Aibot AX20	FLIR Duo R 160 × 120 pixels
Low grass field (2)	July 17, 2019	09:33–9:39	40 m	Leica Aibot AX20	FLIR Duo R 160 × 120 pixels
Low grass field (3)	July 31, 2019	08:13–08:22	40 m	Leica Aibot AX20	FLIR Duo R 160 × 120 pixels
Abenteuer Affenberg (1)	August 22, 2019	06:16–07:12	70 m	DJI Mavic Pro	FLIR Duo R 160 × 120 pixels
Alvarado Creek (1)	January 30, 2020	16:05–17:19	60 m, 80 m	Action Drone ADH	FLIR Vue Pro 336 × 256 pixels $f = 6.8$ mm
Alvarado Creek (2)	March 4, 2020	08:00–08:44	60 m, 80 m	Action Drone ADH	FLIR Vue Pro R 640 × 512 pixels $f = 13$ mm
Abenteuer Affenberg (2)	May 14, 2020	09:00–09:50	120 m	Leica Aibot AX20	WIRIS Pro 640 × 512 pixels $f = 35$ mm
Abenteuer Affenberg (3)	May 19, 2020	09:00–10:00	120 m	Leica Aibot AX20	WIRIS Pro 640 × 512 pixels $f = 35$ mm
Abenteuer Affenberg (4)	February 17, 2021	13:00–14:00	150 m	Leica Aibot AX20	WIRIS Pro 640 × 512 pixels $f = 35$ mm Sony ILCE-7RM2

to align sequential images using RSI approaches and is beneficial for SfM processing, by enabling a high number of match points to be identified, which are then used in the 3D point cloud and orthomosaic generation.

The first UAV imaging mission was conducted at the monkey park on May 19, 2020 between 09:00 and 10:00. At the time this flight was conducted, 162 Japanese macaques (*Macaca fuscata),* including $N=73$ sexually mature females (≥ 3.5 years), $N=52$ sexually mature males (≥ 4.5 years), and $N=37$ immature individuals were present in the park. The second UAV imaging mission was conducted at the monkey park on February 17, 2021, between 13:00 and 14:00. At the time this flight was conducted, 163 Japanese macaques (*Macaca fuscata)* were present within the monkey park, including $N=75$ sexually mature females (≥ 3.5 years), $N=54$ sexually mature males (≥ 4.5 years), and $N=34$ immature individuals.

Within the four-hectare enclosure, the monkeys are kept under (semi-) free conditions and are not hindered from any social interactions with group members. Visitors have access to the population from the beginning of April to the beginning of November via guided tours. Guided tours lead the visitors through one-third of the whole enclosure along a marked path (visible in Fig. 2a). Visitors are not allowed to feed, touch, or interact with the animals. The remaining parts of the forest area are only accessible by the monkeys and offer withdrawal possibilities for the animals (Fig. 2).

The vegetation within the monkey park is a natural mixed forest, which includes *Corylus avellana*, *Oxalis spp.*, *Petasites spp.*, *Pinus sylvestris*, *Poaceae*, *Rubus*

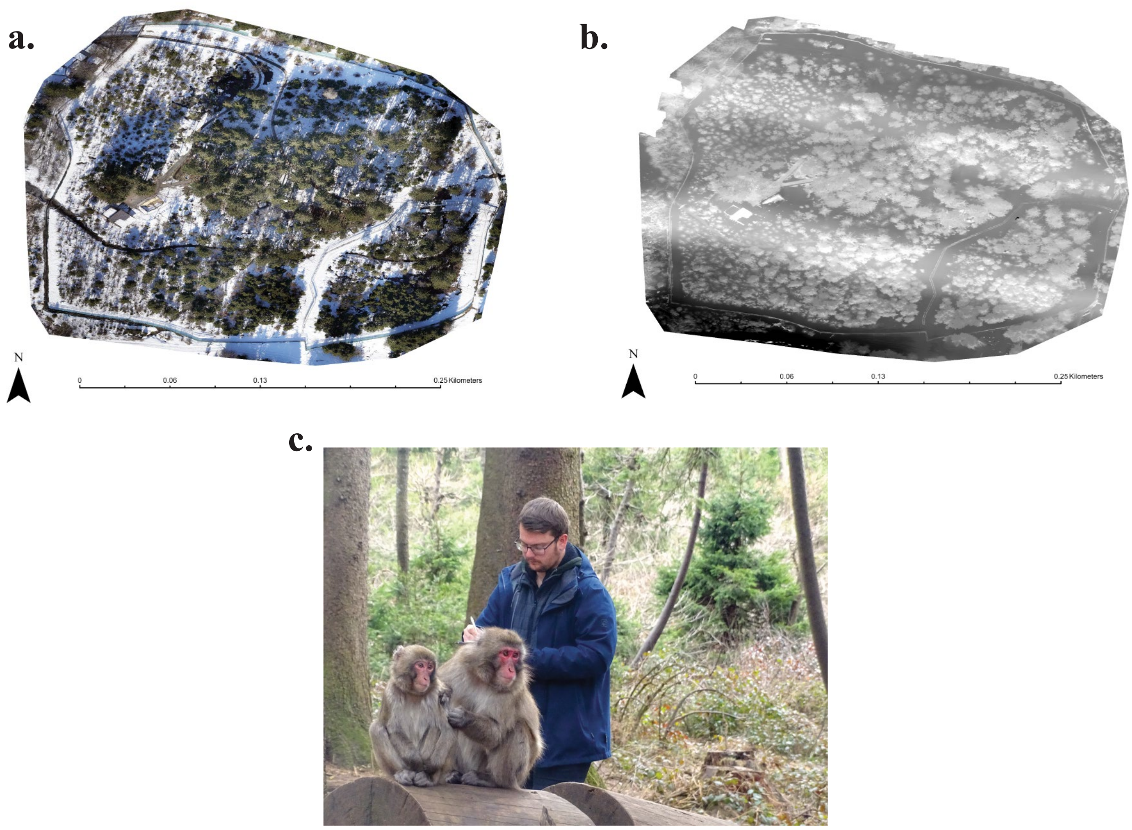

Fig. 2 RGB orthomosaic (**a**) and TIR orthomosaic (**b**) of the Affenberg study area in Landskron, Austria. Gray tones in the TIR image indicate relative brightness temperatures from cool (dark) to warm (light). A researcher next to two monkeys to give an idea of scale (**c**). Fully grown Japanese macaques are typically 52–57 cm in length

idaeus, *Salix spp.*, *Sambucus nigra*, and *Urtica spp.* which are trees common in southern Austria (Pflüger et al., 2021). The dominant species is tall spruce (*P. abies*) which can reach a height of 30 m. The central area of the park consists of sparse forest with grassland clearings and bare ground. The periphery area consists of forested slopes with densely vegetated ground-level shrubs and swamp areas. The monkey park also includes a small natural stream that runs through the enclosure. This area has a Central European Climate that has four distinct seasons, including hot and moderately wet summers and long harsh winters where there is frequent snow cover, and the temperature often drops below freezing.

The May 2020 UAV imaging mission at the monkey park was conducted with a Leica Aibot AX20 equipped with the WIRIS Pro sensor, which collects both TIR and RGB imagery simultaneously at a resolution of 640 × 512 pixels, with a focal length of 35 mm and 1920 × 1080 pixels with a focal length of 3.5 mm, respectively. Images were captured at a height of 120 m AGL (90 m above max canopy height). Flight speed was 2 m s^{-1} and an image trigger interval of 1 s. The TIR images collected have a GSD of 0.05 m.

The same TIR imager was used for the February 2021 mission and was supplemented with a high-resolution Sony ILCE-7RM2 RGB camera with a focal length of 55 mm. Imagery from the RGB camera was used as reference data to validate monkey detections based on the TIR imagery and provide scene context. Images were captured from a height of 150 m above ground level with a flight speed of 5 m s^{-1}. The TIR images have a GSD of 6.78 cm, while the GSD of the RGB images is 1 cm.

Animal reaction testing

During pre-imaging testing and imaging flights conducted over Affenberg, the Japanese macaques were closely monitored by staff members of the park for any signs of negative reactions and stress behavior. According to the primate experts at the park, if the monkeys perceived the UAV as a threat, they would have fled toward the wooded areas of the enclosure, ascended into the trees and mothers would have drawn juveniles close to them. Additionally, alarm calls would have been vocalized, individuals would have shown increased vigilance, and/or the monkeys would have started to show stress behavior such as autogrooming, scratching, yawning, and/or shaking while repeatedly focusing on the stressor and after the stressor was gone (post-conflict reactions) (Kutsukake & Castles, 2001; Schino et al., 1988). A trained observer from the facility was situated within the park to assess whether the monkeys reacted to flights conducted at 120 m altitudes with a Leica Aibot AX20 hexacopter that emits a loud buzzing sound in-flight. The dimensions of the UAV with unfolded frame arms and GPS mount are 167 × 152 × 759 cm. Take-off and landing point for the UAV was selected to be > 100 m from the edge of the inhabited area of the monkey compound to allow for the UAV to achieve flight altitude before imaging commenced overhead.

Image differencing and movement detection

For image alignment and co-registration based on the RSI approach, the TIR image pairs from the 19 May 2020 study site were processed using a program called IMPP, which uses the oriented FAST and rotated BRIEF (ORB) (Rublee et al., 2011) for object recognition. IMPP was run on contrast-enhanced TIR grayscale images using contrast limited AHE (CLAHE). CLAHE is a type of region-based adaptive contrast equalization where contrast amplification is limited, which reduces the problem of noise amplification (Ritika & Kaur, 2013). Transformation matrices were applied to warp the second TIR image of a time-sequential RSI pair to the previously captured image.

Co-aligned RSI pairs were enhanced to highlight moving monkeys by first applying histogram matching to the image pairs and then image differencing. Histogram matching was used for image-to-image radiometric normalization to reduce the effects of inherent brightness temperature variations between image flights and enable pixels exhibiting substantial image brightness changes to be emphasized. These enhanced pixels correspond to targets in motion during the capture of sequential image frames. Differenced images were also created, which provided images that highlighted areas of change within the scene, which were primarily brightness anomalies associated with monkeys in motion between the sequential image capture.

Structure from motion processing

SfM image processing was implemented to generate 3D point clouds and surface models from the overlapping TIR images collected from the February imaging flight. The model was then utilized to create orthorectified images and orthomosaics. Agisoft Metashape Professional version 1.7.3 was used to process the TIR and RGB image sets. We first selected images for alignment and removed unwanted images (blurry images, images taken before the UAV had reached altitude, images outside of the study area). Once the final image sets were established, the selected images were aligned, camera position and orientation for each image were estimated and a sparse point cloud model was generated. Following this, camera optimization was performed, and error reduction measures were taken by removing points with either high reconstruction uncertainty, high projection error, or low projection accuracy as outlined in the Agisoft PhotoScan Workflow released by the USGS National UAS Project Office (USGS, 2017). The estimated camera altitude information, which is the distance of the scene object from the camera station, was calculated for each camera station and combined to generate a dense point cloud. From this dense point cloud, a 3D polygon mesh model was derived and is a representation of the surface through the connection of vertices, edges, and faces. After this surface was generated, the orthomosaic image was applied over the polygon mesh model, which links elevation data to its corresponding points in the image and creates a 3D visual representation of the surface. Three-dimensional models from the TIR images were compared with those from higher spatial resolution RGB images to see how well they aligned. Digital surface models (DSM) derived from the RGB and TIR point clouds for each dataset were exported to ArcGIS Pro 2.8.1, and the difference between them was calculated (e.g., TIR-RGB) to determine similarities and inconsistencies between the two products. Orthomosaics were generated from both the RGB imagery and TIR imagery sets for the Affenberg study site (Fig. 1a, b). The TIR orthomosaic was created using the maximum value from each set of overlapping images for an area, increasing the probability that monkeys visible in individual images would be visible in the overall mosaic.

Japanese macaques were visually detected and manually delineated using both the TIR image frames and TIR orthomosaic images. All analyses were limited to the spatial extent of the TIR image, which was considerably smaller than the extent of the RGB image. Monkey detections were categorized as: (1) being evident in both RGB and TIR, (2) image objects that indicated likely monkey locations in TIR but obscured in RGB, (2) false positives within the TIR imagery, (3) groups of multiple adjacent monkeys presenting as one object within the TIR imagery, and (4) monkeys visible in RGB but not TIR imagery, as summarized in Table 2. Monkeys appeared as spatial clusters or objects of contiguous pixels having TIR digital numbers (DNs) that were at least 19% greater than the land surface and were marked as apparent monkey locations. Monkeys identified within the TIR imagery were then validated through interpretation of the simultaneously captured February 2021 RGB imagery to determine if monkey detections from the February 2021 TIR image sets were reliable. After this analysis was conducted, the February 2021 RGB imagery was visually interpreted to determine if any monkeys were visible within the RGB imagery that was not present in the TIR imagery. The TIR images had a larger ground sampling distance than the RGB imagery and image analysis was limited to this smaller spatial extent where scene coverage coincided. Each TIR-RGB image frame pair was analyzed, and monkeys were counted regardless of

Table 2 Accuracy assessment results based on February 2021 Affenberg image set. Number of image-based detections within the individual frames of TIR imagery relative to those from individual RGB image frames

	Hot spots interpreted as monkeys from TIR images	% of total visible monkeys in TIR images
Monkeys visible in RGB and TIR	187	67.3%
Hot spots identified as monkeys in TIR but obscured in RGB	76	27.3%
Scene objects misidentified as monkeys	15	5.4%
Total	278	100%

whether they had previously been counted in sequential or parallel image frames. This was done to establish detection accuracy rather than attempting to conduct an overall population count. Monkey counts were conducted directly from each TIR/RGB orthomosaic image.

Results

Pre-mission sensor and platform testing

The most important consideration for successful monkey detection is to capture images when there is sufficient thermal contrast between monkeys' surface temperature and their background (i.e., ground and vegetation canopy) temperatures. This is easier to achieve in the early morning or during winter when air temperatures are cooler (between 7.7 and 11.2 °C for this study). While thermal contrast may be sufficient in the early afternoon during the winter, as demonstrated in this study, a disadvantage is that scene objects (rocks, paths, exposed areas of trees, patches of earth, etc.) not covered in snow may exhibit warmer surface temperatures and therefore TIR signatures, which can yield thermal anomalies that may be mistaken for monkeys (more on this below).

Another vital consideration when ensuring consistent monkey detection is to maintain a UAV flight height and camera focal length that results in the GSD being at least half and ideally much smaller than the size of the viewable portion of the monkey, which is dependent on monkey size and orientation. Monkeys walking or laying down tend to have larger visible surface areas than monkeys sitting or climbing in trees. Monkey length measurements taken from thermal imagery ranged from 35 cm when seated to 56 cm when walking and fully extended.

Flight speed, camera trigger rate, and altitude above ground level are site-dependent and should be based on the scene's terrain characteristics, the movement speed of the animal being monitored, and the image analysis approach implemented. With both the camera and the subject in motion, the image capture interval must be fast enough to capture an animal that is in motion and can be moving in and out of canopy cover and might not be visible from one image frame to the next.

Animal reaction

The monkeys at Affenberg appeared to be aware of and occasionally looked up at the UAV when flying at 150 m AGL but did not exhibit obvious signs of stress, neither during nor immediately after the test session (post-conflict reaction). Stress indicators such as alarm calls, scratching, ascending into the trees, or any other stress behaviors were not demonstrated, and animal experts inferred that the monkeys did not consider the UAV to be an imminent threat. The only reaction observed was monkeys glancing up at the UAV on the initial flyover as the UAV approached and the noise increased. After spotting the source of the noise, they immediately continued their previous behaviors, e.g., sleeping on the ground, grooming, foraging, or playing (more on this below). Subsequently, they paid even less attention to the UAV on the following passes, as they seemingly became accustomed to the noise.

Monkey identification within individual images

Of the 374 TIR images collected over the study area for the February 2021 mission, 94 images contain monkeys that are clearly detectable. Within these 94 images, 278 monkeys were detected. The 94 corresponding high-spatial resolution RGB images were also interpreted to detect monkeys and were used as reference data to assess the accuracy of monkey detections from UAV-TIR images having coarser spatial resolution. Two hundred thirty-five (235) monkeys were detected within the RGB imagery. Of the 278 likely monkeys detected in the TIR images, 187 were confirmed with the RGB imagery, 76 were only observed in the TIR imagery due to being located within vegetation canopies in the RGB images, and 15 had bright (high) TIR signatures that resembled monkeys but were surface objects that were warmed by solar radiation (e.g., rocks, tree stumps, etc.) as shown in Table 2. Of the 235 monkeys visible within the RGB images, 21 were not counted within the corresponding TIR images due to multiple monkeys being huddled together and appearing as one large warm image object, and 27 were visible only in the RGB imagery, as listed in Table 3. These 27 occurrences are associated with monkeys being on the warm roof of a building or path or being in shadows, which limited thermal contrast.

Table 3 Monkeys detected in the individual RGB imagery compared with TIR imagery show that the main source of differences in the number of monkeys located are in areas where there is not sufficient thermal contrast to allow for detection in the TIR imagery

	Identified monkeys in RGB images	% of total visible monkeys in RGB images
Monkeys visible in RGB and TIR	187	79.6%
Monkeys missed due to clustering	21	8.94%
Monkeys visible in RGB but not TIR images	27	11.5%
Total	235	100%

Monkey detection from TIR orthomosaics

Within the orthomosaic generated from the TIR images, 30 monkeys were detected out of a possible 163 Japanese macaques residing in the park, and 16 of these monkeys were also able to be identified within the RGB orthomosaic. The fact this number is substantially lower than monkeys detected from the individual TIR image can be explained not only by the limited potential for repeated counts of the same monkey but also through the orthomosaic process, which can result in the removal of features that are not consistently represented through all overlapping images, such as monkeys in motion or monkeys that are intermittently obscured through canopy cover. Monkeys that were detected in the orthomosaics tended to be monkeys that were seated or who stayed relatively stationary. While this significantly limits the potential for TIR orthomosaics to be used in comprehensive population counts, clusters of monkeys are visible in the TIR orthomosaic, which suggests that sleeping sites could be identified in surveys conducted in the wild.

RSI-based target detection

The images collected in May of 2020 were taken in short interval sequences along the same flight line, which enabled RSI-based target identification. These images were co-registered and georeferenced, and the resulting image pairs were differenced to highlight areas of change corresponding to monkeys in motion. Figure 3 is one of these differenced image pairs and shows two monkeys moving through the scene in consecutive sequential images. The hot spots (shown in white and light gray) in Fig. 3a, b depict the location of monkeys in images taken at one-second intervals. A single monkey appears just above the center of the images in Fig. 3a. In the second image, another monkey enters the view field, and the first shifts lower in the image (Fig. 3b). The differenced image (Fig. 3c) highlights the new position of the monkey and is displayed in yellow, indicating temperature increase (absent then present), and the area that the monkey left is shown in dark purple, indicating cooling (present then absent). Some trees in the scene also exhibit temperature changes likely caused by differences in sun and view angles, transpiration, and foliage movement. These changes are small compared to the temperature changes, associated with monkey movement (presence-absence or absence-presence of monkeys within sequential image frames).

SfM products

Of the 1237 TIR images collected during the February imaging flight, 575 were both situated in the study area and yielded sufficient match points identified to facilitate image alignment and be used for further SfM processing. Camera station position data associated with each image frame allowed for accurate photo alignment and georeferencing without the use of GCPs. The 3D match points automatically created from this dataset were also refined before the final point cloud creation. Points with high reconstruction uncertainty, projection error, or low projection accuracy were removed from the sparse point cloud, which increased the overall accuracy of the model. Figure 4a, b show the number of overlapping images in the Affenberg area and the calculated flight and survey data for both the TIR and RGB imagery.

DSMs were also generated from both the RGB and TIR point clouds and were differenced to create a map (Fig. 4e) that shows the vertical height differences between the two DSM rasters. The observed areas of considerable differences in calculated height

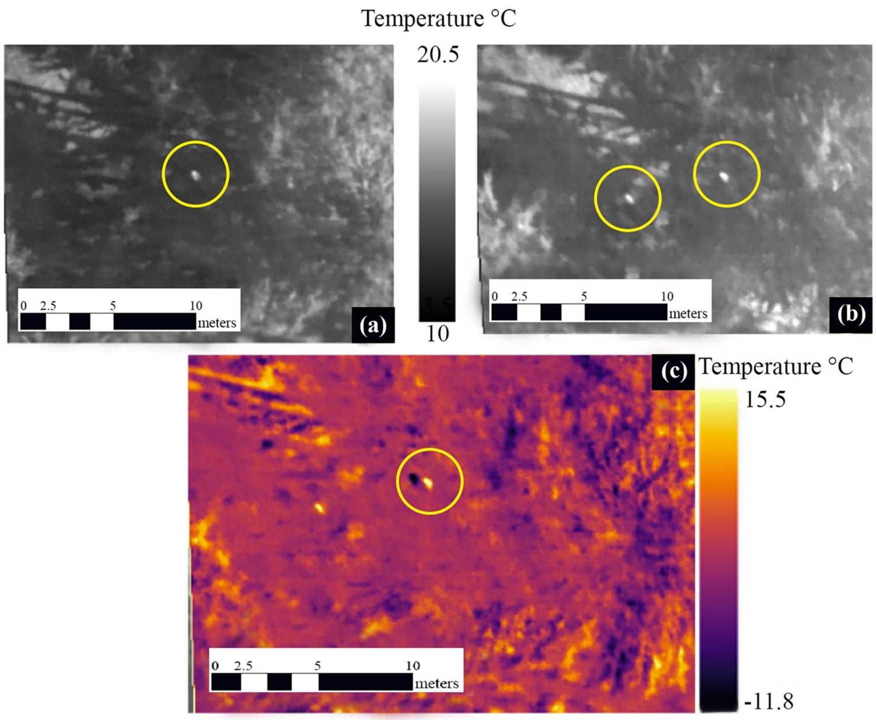

Fig. 3 A comparison of images in a time sequence. The first image (**a**) compared to the second image (**b**) captured at a 1 s interval. In image **a** there is only one monkey present, and then in image **b** a second monkey enters the scene. When the image areas are differenced (**c**) the monkey that moved into the scene shows up more prominently in yellow. Notice that the monkey visible in both frames shifted slightly, as indicated by the cooler area in dark purple close to the monkey furthest to the right

were primarily in densely forested areas, which can be attributed to the differences in how visible and thermal cameras capture vegetation. The gap present in the TIR-derived DSM resulted from a low number of match points having been identified in a densely forested area, which yielded fewer points in the derived point cloud and therefore prevented height estimates in this area.

Target identification within the generated 3D model was also accomplished, with monkeys visible in the orthomosaic also being visible when placed within the 3D scene. However, this is only the case when looking at the coarser 3D polygon mesh and not the more refined dense point cloud. As a result, any elevation estimates taken from these models have the potential for high levels of inaccuracy. No monkeys in this study were able to be identified above ground level in both the TIR and RGB imagery, which prevented any quantitative assessment of the height accuracy of these models.

Discussion

We explored the ability of UAV-TIR systems to conduct wildlife surveys in an arboreal environment. These environments present unique challenges for conventional, ground-based animal surveys because they are typically hard to access and animals within the canopy can be difficult to detect by ground-based observers. UAVs with TIR sensors overcome these limitations by flying over difficult terrain and leveraging the thermal contrast between the warm-bodied animals and their cooler vegetated environments, enhancing detectability, which is in agreement with the finding of Kays et al. (2019) and Burke et al. (2019). Our goal was to address questions pertaining to UAV image capture, processing, and analysis procedures that best enable animal (in our case, monkey) detection. We demonstrated that two novel UAV-TIR image capture and processing approaches facilitate animal detection: (1) rapid-sequence RSI for detecting animals in motion, and (2) SfM applied to UAV-TIR image sets to render 3D models of arboreal animal positions and vegetation canopies.

From the testing of flight and image capture parameters, we determined that UAV flights conducted with the aim of thermal surveillance of wildlife must be planned carefully to ensure flight patterns, speed, height, and time of day are appropriate for the species and terrain being monitored. We used

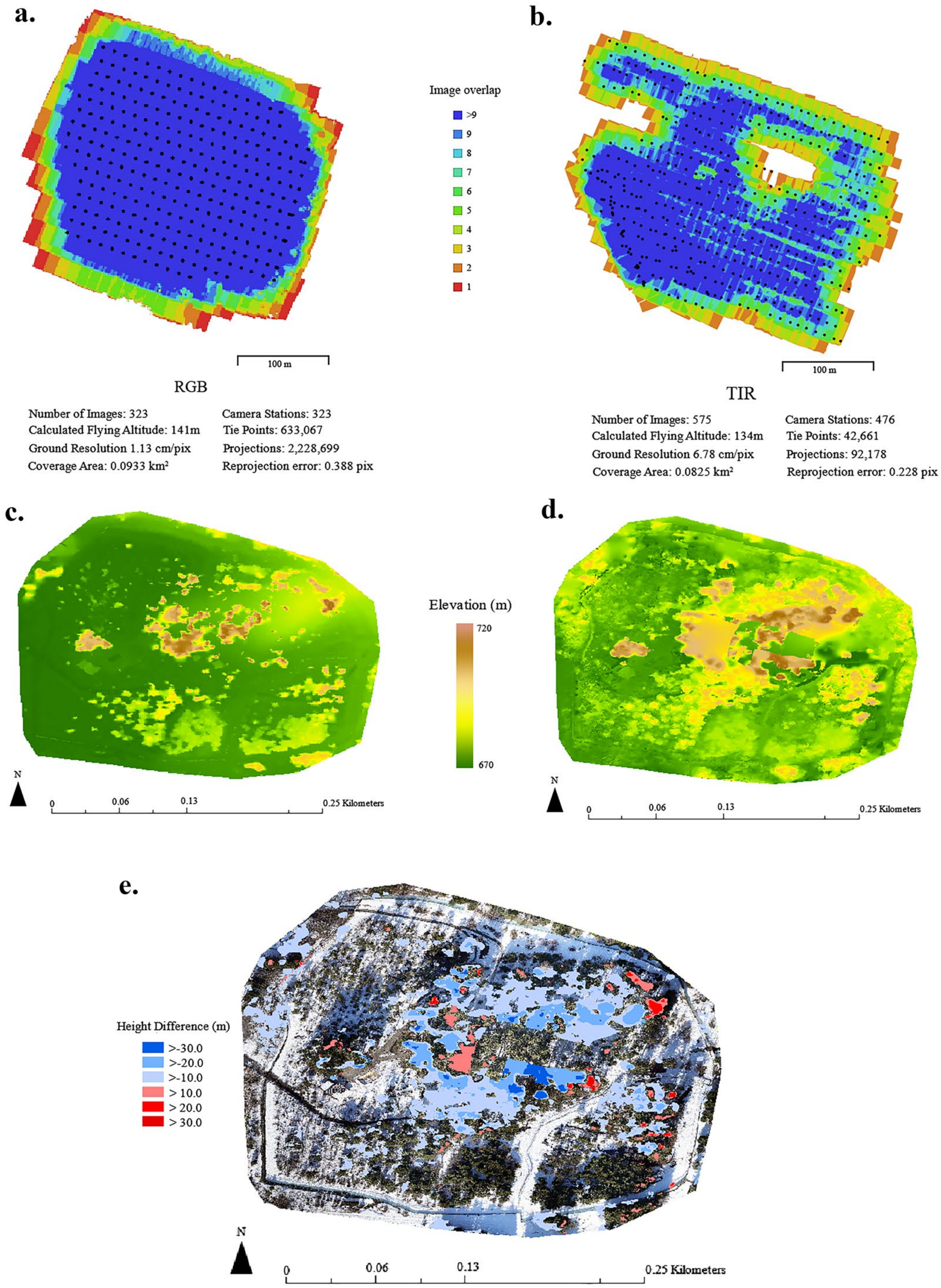

Fig. 4 Flight data for the 2021 February RGB imagery (**a**) and the 2021 February TIR imagery (**b**). The RGB DSM (**c**) and the TIR DSM (**d**) have similar elevation profiles once corrected for consistent differences and are shown in the map (**e**) which is the difference between the RGB and TIR DSMs. Areas with a +/− 10 m height difference are shown in a color gradient indicating RGB was higher (red) or lower (blue) areas with a less than a +/− 10 m difference remain uncolored

"lawnmower" or "racetrack" flight patterns to ensure that there was sufficient image-side overlap to enable RSI and SfM photo alignment. Flight speed and image capture rates were also planned to facilitate a high degree of forward overlap. Synchronizing flight speed, through extension ground speed, and image capture rate is critical for preventing motion blurring and ensuring that clear, interpretable images are collected. Flights conducted at 150 m AGL with a flight speed of 1 m s^{-1} and an image capture interval of 1 s provided high-quality TIR images that allowed for the detection of thermal targets.

The time of day for conducting imaging flights is an important consideration and thermal imaging should be executed when the background environment is considerably cooler than the targets of interest, which are typically in the early morning, at night, or during the winter, which is consistent with the finding of Burke et al. (2019) and Kays et al. (2019), although both articles focused on daily variability rather than seasonal variability. Flying at night increases the visibility of mammals (Kays et al., 2019), but comes with significant challenges. One of the challenges with flying at night is that it is more carefully regulated and requires special permission to conduct. Night flights also limit the ability to simultaneously collect RGB imagery, which provides valuable scene information and can be used to validate target locations and prevent false positives. For these reasons, flights were conducted in the early morning and during the winter months.

The selection of flight altitudes should be based on camera focal length and the projected size of targets being monitored when viewed from the nadir. The image GSD based on flight altitude AGL and camera focal length should be at or less than half the target to ensure detection. For this study, the maximum TIR GSD was 17% of the size of the targets. Another consideration is the disturbance of the animals being monitored and their sensitivity to the sight and sound of UAV platforms. Higher flight altitudes with longer focal length lenses should be utilized to prevent adverse reactions from the animals. Flying at too low of an altitude might impact the overall reliability of the study if the animals being monitored flee from the approaching UAV, negatively impacting target detection. Monkey reaction to the overflying UAV in this study appeared to be minimal when flown at 70 m AGL with a DJI Mavic Pro and at 120 m with a Leica Aibot AX20 UAV, and the monkeys did not exhibit any of the behavioral responses seen in Pomeroy et al. (2015). Staging the take-off and landing points at least 100 m from the study area seems to have limited animal stress and insured that the UAV was at a safe altitude before coming into view of the monkeys and is the minimum staging distance recommended by Mulero-Pázmány et al. (2017). These results might not be indicative of the reaction to UAVs from monkeys in the wild because of the Affenberg monkeys' habituation to human presence, which may have worked to desensitize them to anthropomorphic noises. Altitudes identified in this study may be used as the lower bound for acceptable flight attitudes and may need to be increased in a true wilderness setting.

Monkeys were detected in 94 out of the 374 TIR image frames collected over the park, with a total of 278 apparent monkey objects. The number of detected monkeys is greater than the overall monkey population in the park because highly overlapping images result in the possibility of the same monkey being counted within multiple image frames. Out of 278 image objects consisting of pixels with significantly higher thermal signatures than the surrounding environment, 187 were positively identified as monkeys within the RGB imagery, with 76 not being apparent in the RGB imagery. This discrepancy represents omission errors with the RGB imagery because of camouflage by the vegetation background or canopy obstructions or commission errors from confusion with warm objects other than monkeys. Only 15 of the detected image objects were false positives. The RGB imagery was useful in differentiating multiple monkeys huddled in groups that were portrayed in the TIR imagery as a single warm object, as well as for detecting smaller monkeys whose TIR image signatures were too small or cool to be readily detectable. Within the TIR orthomosaic generated for the Affenberg study area, 30 monkeys were detected. This number is significantly lower than the monkeys visible within the individual TIR images because the image mosaicking process used to create the orthoimage selects pixel values based on consistency between image frames and results in the omission of monkeys that are moving or inconsistently visible within overlapping images.

Many of the monkeys that were readily detected through interpretation of the TIR imagery are poorly or non-detectable on the RGB imagery, as the monkey's visible signature was often confused with rocks or obscured by shadows or vegetation. The contrast between a monkey (target) and its surrounding environment (background) provided by TIR imagery was generally suitable for detecting monkeys and did not require cross-checking RGB imagery, which is a laborious task. Based on interpretation of the TIR imagery, we were able to detect 80% of monkeys positively detected in the RGB imagery, as well as an additional 76 monkeys that were not detectable from the RGB images. Only 5.4% of thermal hotspots were confirmed to be incorrectly detected as monkeys, which increases confidence that the 76 hotspots not validated in the RGB imagery were indeed monkeys. These results show that TIR imagery enabled higher detection levels compared to RGB imagery while still having low levels of false detections and monkey omissions.

The RSI technique, where rapid sequence images are captured, co-registered, and subjected to image differencing was found to be effective for detecting monkeys that were in motion during image capture. The absence-presence or presence-absence of monkeys in motion for fixed pixel positions were manifest as large changes in TIR radiance values, as represented by image difference signatures.

Using TIR imagery to create 3D models through SfM processing proved to be moderately successful. The Affenberg TIR point cloud and 3D polygon mesh appeared to represent the general structure of the terrain and vegetation well but did not have the definition and point density of the RGB models (similar to the findings in Webster et al., 2018). Dense point clouds derived from the TIR imagery portray thermal targets but lacked the necessary density of target points to accurately identify the targets and represent the 3D structure of vegetation canopies. 3D polygon meshes derived from these point clouds increased the interpretability of the targets through a smoothing process but decreased the overall potential accuracy.

Conclusions

TIR imagery from UAV platforms increases the efficiency and ability to detect warm-bodied animals in arboreal environments and makes targets more readily detectable within complex scenes. The RGB images can help to validate target identification, but many targets would easily be overlooked if it was the only source of imagery. RGB imagery also helps prevent false detections, which was a challenge for this study because the difference between scene objects surrounded by snow created a contrast that could be mistaken for a monkey and is only identifiable with previous knowledge of the scene or through checking validity using the supplemental RGB images.

Challenges associated with repeat-pass RSI testing include the lack of GNSS-based image triggering, which is recommended for precise RSI image capture and would increase the replicability of camera stations and view geometries between imaging flights. Future research should include conducting UAV-TIR surveys using repeat-pass flight lines with GNSS-based image triggering to see how the precise matching of imaging stations impacts the accuracy of image registration and change detection associated with monkeys that moved position between flight passes. The use of RSI-based change detection can provide information on animal movement, and future research could test its applicability to animal tracking.

A challenge associated with morning TIR imaging flights is substantial changes in environmental temperatures as the sun rises and the scene warms. This modifies background-target temperature differences over time and can limit the consistent detectability of targets. It also reduces the effectiveness of RSI change detection through image differencing. As a scene warms, repeat pass images can have very different temperature differences, which could register as false positives and make it difficult to uniquely identify moving animals.

The 3D models generated from SfM processing can give insight into animal behavior by detecting animals within the canopy and providing height estimations. Future research should explore ways of increasing point density within the point cloud, which would allow for direct animal elevation measurements from this model and increase height estimation accuracy.

Once TIR imaging procedures are refined and arboreal animals can be detected accurately and consistently, future research could emphasize the detection of species in mixed-species habitats based on thermal, shape, and size signatures. We recommend that further research on UAV tolerance be conducted by varying flight height and UAV type in a systematic manner.

Acknowledgements This work was supported by the National Science Foundation under the Dynamics of Coupled Natural and Human Systems program (BCS-1826839). Any opinions, findings, conclusions, or recommendations expressed in this material are those of the authors and do not necessarily reflect the views of the National Science Foundation. Support was also provided from the San Diego State University for a research stipend and the Austrian Marshall Plan Foundation for supporting travel and data collection. Ulf Scherling from CUAS for performing the UAV mission at Affenberg. Affenberg Landskron and the manager of the park, Svenja and Peter Gaubatz, and the animal care staff who provided access and support for our surveys over the monkey park.

Data availability The datasets generated during and/or analyzed during the current study are available from the corresponding author on reasonable request.

Declarations

Ethics approval The authors declare no competing interests.

References

Burke, C., Rashman, M. F., Longmore, S. N., McAree, O., Glover-Kapfer, P., Ancrenaz, M., & Wich, S. A. (2019). Successful observation of orangutans in the wild with thermal-equipped drones. *Journal of Unmanned Vehicle Systems, 7*(3), 235–257. https://doi.org/10.1139/juvs-2018-0035

Campbell, G., Head, J., Junker, J., Nekaris, K. A. I., Wich, S., & Marshall, A. (2016). Primate abundance and distribution: Background concepts and methods. An introduction to primate conservation, pp.79–110.

Coulter, L. L., Stow, D. A., Lippitt, C. D., & Fraley, G. W. (2015). Repeat station imaging for rapid airborne change detection. In C. D. Lippitt, D. A. Stow, & L. L. Coulter (Eds.), Time-sensitive remote sensing (pp. 29–43). Springer. https://doi.org/10.1007/978-1-4939-2602-2_3

Ditmer, M. A., Vincent, J. B., Werden, L. K., Tanner, J. C., Laske, T. G., Iaizzo, P. A., Garshelis, D. L., & Fieberg, J. R. (2015). Bears show a physiological but limited behavioral response to unmanned aerial vehicles. *Current Biology, 25*(17), 2278–2283. https://doi.org/10.1016/j.cub.2015.07.024

Gonzalez, L. F., Montes, G. A., Puig, E., Johnson, S., Mengersen, K., & Gaston, K. J. (2016). Unmanned aerial vehicles (UAVs) and artificial intelligence revolutionizing wildlife monitoring and conservation. *Sensors, 16*(1), 97. https://doi.org/10.3390/s16010097

He, G., Yang, H., Pan, R., Sun, Y., Zheng, P., Wang, J., Jin, X., Zhang, J., Li, B., & Guo, S. (2020). Using unmanned aerial vehicles with thermal-image acquisition cameras for animal surveys: A case study on the Sichuan snub-nosed monkey in the Qinling Mountains. *Integrative Zoology, 15*(1), 79–86. https://doi.org/10.1111/1749-4877.12410

Kays, R., Sheppard, J., Mclean, K., Welch, C., Paunescu, C., Wang, V., Kravit, G., & Crofoot, M. (2019). Hot monkey, cold reality: Surveying rainforest canopy mammals using drone-mounted thermal infrared sensors. *International Journal of Remote Sensing, 40*(2), 407–419. https://doi.org/10.1080/01431161.2018.1523580

Kutsukake, N., & Castles, D. L. (2001). Reconciliation and variation in post-conflict stress in Japanese macaques (Macaca fuscata fuscata): Testing the integrated hypothesis. *Animal Cognition, 4*(3–4), 259–268. https://doi.org/10.1007/s10071-001-0119-2

Loerch, A., Paulus, G., & Lippitt, C. (2018). Volumetric change detection with using structure from motion – The impact of repeat station imaging. *Gi_forum*. https://doi.org/10.1553/giscience2018_01_s135

Mulero-Pázmány, M., Jenni-Eiermann, S., Strebel, N., Sattler, T., Negro, J. J., & Tablado, Z. (2017). Unmanned aircraft systems as a new source of disturbance for wildlife: A systematic review. *PLoS ONE, 12*(6), e0178448. https://doi.org/10.1371/journal.pone.0178448

Oishi, Y., Oguma, H., Tamura, A., Nakamura, R., & Matsunaga, T. (2018). Animal detection using thermal images and its required observation conditions. *Remote Sensing, 10*(7), 1050. https://doi.org/10.3390/rs10071050

Pflüger, L. S., Pink, K. E., Wallner, B., Radler, C., Dorner, M., & Huffman, M. A. (2021). Twenty-three-year demographic history of the Affenberg Japanese macaques (Macaca fuscata), a translocated semi-free-ranging group in southern Austria. *Primates; Journal of Primatology, 62*(5), 761–776. https://doi.org/10.1007/s10329-021-00928-4

Plumptre, A. J., Sterling, E. J., & Buckland, S. T. (2013). *Primate census and survey techniques* (pp. 10–26). A handbook of techniques. Oxford University Press, Oxford.

Pomeroy, P., O'Connor, L., & Davies, P. (2015). Assessing use of and reaction to unmanned aerial systems in gray and harbor seals during breeding and molt in the UK. *Journal of Unmanned Vehicle Systems, 3*(3), 102–113. https://doi.org/10.1139/juvs-2015-0013

Ritika, R., & Kaur, S. (2013). Contrast enhancement techniques for images—A visual analysis. *International Journal of Computer Applications, 64*(17), 20–25. https://doi.org/10.5120/10727-5679

Rublee, E., Rabaud, V., Konolige, K., & Bradski, G. (2011). *ORB: An efficient* alternative to SIFT or SURF. *Proceedings of the IEEE International Conference on Computer Vision*. https://doi.org/10.1109/ICCV.2011.6126544

Schino, G., Scucchi, S., Maestripieri, D., & Turillazzi, P. (1988). Allogrooming as tension-reduction mechanism: A behavioural approach. *American Journal of Primatology, 16*, 43–50. https://doi.org/10.1002/ajp.1350160106

Spaan, D., Burke, C., McAree, O., Aureli, F., Rangel-Rivera, C. E., Hutschenreiter, A., Longmore, S. N., McWhirter, P. R., & Wich, S. A. (2019). Thermal infrared imaging from drones offers a major advance for spider monkey surveys. *Drones, 3*(2), 34. https://doi.org/10.3390/drones3020034

Stow, D. A., Coulter, L. C., MacDonald, G., Lippitt, C. D., McCreight, R., & Zamora, N. (2016). Evaluation of geometric elements of repeat station imaging and registration. *Photogrammetric Engineering & Remote Sensing, 82*(10), 775–788. https://doi.org/10.14358/PERS.82.10.775

Stow, D. A., Tsai, Y. -H., Coulter, L. L., & Lippitt, C. D. (2014). Detecting and measuring moving objects with airborne repeat station imaging in rapid succession mode. *Remote Sensing Letters, 5*(3), 213–220. https://doi.org/10.1080/2150704X.2014.894654

Thiele, S. T., Varley, N., & James, M. R. (2017). Thermal photogrammetric imaging: A new technique for monitoring dome eruptions. *Journal of Volcanology and Geothermal Research, 337*, 140–145. https://doi.org/10.1016/j.jvolgeores.2017.03.022

USGS. (2017). Agisoft PhotoScan workflow. Retrieved May 2020 https://uas.usgs.gov/nupo/pdf/USGSAgisoftPhotoScanWorkflow.pdf

Vas, E., Lescroël, A., Duriez, O., Boguszewski, G., & Grémillet, D. (2015). Approaching birds with drones: First experiments and ethical guidelines. *Biology Letters, 11*(2), 20140754. https://doi.org/10.1098/rsbl.2014.0754

Webster, C., Westoby, M., Rutter, N., & Jonas, T. (2018). Three-dimensional thermal characterization of forest canopies using UAV photogrammetry. *Remote Sensing of Environment, 209*, 835–847. https://doi.org/10.1016/j.rse.2017.09.033

Westoby, M. J., Brasington, J., Glasser, N. F., Hambrey, M. J., & Reynolds, J. M. (2012). Structure-from-motion' photogrammetry: A low-cost, effective tool for geoscience applications. *Geomorphology, 179*, 300–314. https://doi.org/10.1016/j.geomorph.2012.08.021

Witczuk, J., Pagacz, S., Zmarz, A., & Cypel, M. (2018). Exploring the feasibility of unmanned aerial vehicles and thermal imaging for ungulate surveys in forests—Preliminary results. *International Journal of Remote Sensing, 39*(15–16), 5504–5521. https://doi.org/10.1080/01431161.2017.1390621

Zhang, H., Wang, C., Turvey, S. T., Sun, Z., Tan, Z., Yang, Q., Long, W., Wu, X., & Yang, D. (2020). Thermal infrared imaging from drones can detect individuals and nocturnal behavior of the world's rarest primate. *Global Ecology and Conservation, 23*, e01101. https://doi.org/10.1016/j.gecco.2020.e01101

Zheng, H., Zhong, X., Yan, J., Zhao, L., & Wang, X. (2020). A thermal performance detection method for building envelope based on 3D model generated by UAV thermal imagery. *Energies, 13*(24), 6677. https://doi.org/10.3390/en13246677